



Published in final edited form as:

*J Neurooncol.* 2014 December ; 120(3): 539–546. doi:10.1007/s11060-014-1583-2.

## Combining Diffusion and Perfusion Differentiates Tumor from Bevacizumab-Related Imaging Abnormality (BRIA)

Nikdokht Farid, M.D.<sup>1,6</sup>, Daniela B. Almeida-Freitas, M.D.<sup>1,2,6</sup>, Nathan S. White, Ph.D.<sup>1,6</sup>, Carrie R. McDonald, Ph.D.<sup>3,6</sup>, Joshua M. Kuperman, Ph.D.<sup>1,6</sup>, Abdulrahman A. Almutairi, M.D.<sup>1,6</sup>, Karra A. Muller, M.D., Ph.D.<sup>4</sup>, Scott R. VandenBerg, M.D., Ph.D.<sup>4</sup>, Santosh Kesari, M.D., Ph.D.<sup>5,7</sup>, and Anders M. Dale, Ph.D.<sup>1,3,5,6</sup>

<sup>1</sup>Department of Radiology, University of California, San Diego 200 West Arbor Drive, MC 0834, San Diego, CA 92103-0834

<sup>2</sup>Department of Radiology, University of Sao Paulo, Brazil Largo São Francisco, 95 - Centro, São Paulo, 01005-010, Brazil

<sup>3</sup>Department of Psychiatry, University of California, San Diego 9500 Gilman Drive, MC 0603, La Jolla, CA 92093-0603

<sup>4</sup>Department of Pathology, University of California, San Diego 9500 Gilman Drive, La Jolla, CA 92093

<sup>5</sup>Department of Neurosciences, University of California, San Diego 9500 Gilman Drive, La Jolla, CA 92093-0662

<sup>6</sup>Multimodal Imaging Laboratory, University of California, San Diego 8950 Villa La Jolla Drive, Suite C101, La Jolla, CA 92037

<sup>7</sup>Translational Neuro-Oncology Laboratories, Moores Cancer Center, UC San Diego 3855 Health Sciences Drive, La Jolla, CA 92093

---

### Introduction

Malignant glioma is the prototypical example of a highly vascularized tumor, with pathological angiogenesis largely attributable to vascular endothelial growth factor (VEGF). As a result, there has been a great deal of interest in the development and evaluation of anti-VEGF agents, such as bevacizumab, in the treatment of recurrent GBM.<sup>1</sup> More recently, investigators have also started to evaluate the efficacy of anti-VEGF agents in the treatment of brain metastases,<sup>2</sup> particularly brain metastases from non-small cell lung cancer (NSCLC).<sup>3</sup> With the increasing use of antiangiogenic agents in the treatment of high-grade gliomas and to a lesser extent in the treatment of brain metastases, we are becoming increasingly aware of distinctive imaging findings seen in patients treated with these agents.

---

Address for correspondence: N. Farid, Department of Radiology; 200 West Arbor Drive #8756; San Diego, CA 92103; phone: 858-837-0744; fax: 858-558-5775; nfarid@ucsd.edu.

Conflicts of interest: None of the authors have any personal or institutional financial interest in drugs, materials, or devices described in this submission.

The phenomenon of “pseudoresponse” is well documented and refers to a marked decrease in contrast enhancement and edema on MR imaging that often occurs after the initiation of bevacizumab therapy, without significant effect on overall survival.<sup>4</sup> This pseudoresponse is attributed to normalization of the blood-brain barrier. Another interesting phenomenon is the development of regions of marked and persistent restricted diffusion in a subset of patients with malignant glioma and brain metastases after starting bevacizumab therapy. Figure 1 illustrates this bevacizumab-related imaging abnormality (BRIA) in a patient with brain metastasis from NSCLC. As expected, the degree of contrast enhancement and the surrounding FLAIR hyperintensity significantly decrease on the 6 month follow-up scan after initiation of bevacizumab. However, a region of marked restricted diffusion appears just 1 month after initiating bevacizumab, increases in size on the 6 month follow-up scan, and persists at 12 months.

Previous studies have described this phenomenon in a subset of patients with malignant glioma.<sup>5-7</sup> Histopathologic data from these studies showed “atypical gelatinous necrosis” and fibrotic, hyalinized blood vessels in the regions of restricted diffusion rather than viable tumor. Furthermore, these lesions have been correlated with improved survival.<sup>6</sup> However, based on standard MR imaging, differentiating these lesions from areas of viable tumor, which are also associated with restricted diffusion,<sup>8,9</sup> remains challenging. Although prior studies have suggested that the degree of diffusion restriction within these lesions as well as hypoperfusion on DSC perfusion imaging may help to distinguish these lesions from recurrent tumor,<sup>6,7</sup> there has been no systematic comparison of the diffusion and perfusion characteristics of these lesions to known tumor.

Furthermore, whereas prior studies have evaluated these areas of restricted diffusion using standard DWI and ADC, we employ Restriction Spectrum Imaging (RSI), an advanced DWI technique that maximizes sensitivity to the restricted diffusion signal within cells while excluding the hindered diffusion signal associated with edema.<sup>10</sup> We have previously shown that RSI offers improved tumor conspicuity relative to high b-value ADC in patients with primary and metastatic brain tumors.<sup>11</sup> We have also shown that it is less influenced by bevacizumab-induced decreases in FLAIR hyperintensity than standard ADC and therefore may serve as a more robust biomarker of tumor cellularity in the setting of pseudoresponse.<sup>12</sup> Given these previous findings, we evaluate whether RSI, like DWI, demonstrates marked and persistent restricted diffusion in a subset of patients treated with bevacizumab.

In the current study, we perform a systematic comparison between patients with BRIA and those with treatment-naïve high-grade glioma in order to determine whether the degree of restricted diffusion and the rCBV can help to differentiate between these entities. We hypothesize that by using RSI and DSC perfusion in combination, we will be able to reliably differentiate between BRIA and recurrent tumor.

## Materials and Methods

### Patients

All patients included in the study signed consent forms approved by the institutional review board. Medical records of 191 patients with high-grade glioma (i.e. WHO grade III or IV) or brain metastases, who had undergone MR imaging with a standardized brain tumor protocol at UCSD Moore's Cancer Center between December 2010 and June 2013, were reviewed. Of those 191 patients, 67 (35%) had received bevacizumab therapy at some point during their treatment regimen, in addition to standard chemotherapy and radiation. After initiating bevacizumab therapy, eight (12%) of these 67 patients developed regions of marked restricted diffusion which persisted on at least 2 sequential MRI's, with the restricted diffusion persisting on average 8 months and up to 16 months in duration. Four patients had GBM, 2 had anaplastic astrocytoma, and 2 had brain metastases. The average age of this final cohort was 55 years, ranging from 29 to 79 years, with 5 males and 3 females (Table 1). In addition, 6 patients with GBM were selected as treatment naïve controls (i.e. no surgery, no chemotherapy, and no radiation at the time of initial imaging) in order to establish the baseline diffusion and perfusion characteristics of known tumor. The average age of the GBM controls was 70 years, ranging from 52 to 85 years, with 3 males and 3 females.

### MR Imaging

MR imaging was performed on a 3.0T GE Signa Excite HDx scanner equipped with an 8-channel head coil. Our imaging protocol included pre- and post-Gadolinium 3D volumetric T1-weighted IR-SPGR sequences (TE/TR = 2.8/6.5ms; TI = 450ms; FA = 8°; FOV = 24cm; 0.93×0.93×1.2mm) and a 3D T2-weighted FLAIR sequence (TE/TR = 126/6000ms; TI = 1863ms; FOV = 24cm; 0.93×0.93×1.2mm).

RSI was available for all patients and controls in the study and was obtained using a single-shot pulsed-field gradient spin-echo (PGSE) echo-planar imaging (EPI) sequence (TE/TR = 96ms/17s; FOV = 24cm, matrix = 96×96×48) with 4 *b*-values (*b* = 0, 500, 1500, and 4000 s/mm<sup>2</sup>), and 6, 6, and 15 unique diffusion directions for each non-zero *b*-value, respectively (28 total volumes, ~8 min scan time).

DSC perfusion was available for 6 of the patients with BRIA and for 4 of the GBM controls. Using a gradient-echo EPI sequence (TE/TR = 35/1600 ms; FA = 90°; section thickness 5 mm with intersection gap of 1 mm; 22 sections; matrix 96 × 96), 20 mL of gadobenate dimeglumine (Gd-BOPTA; 0.1 mmol/kg body weight; Multihance, Bracco Imaging) was injected intravenously with an MR-compatible power injector at a rate of 3 mL/s through an antecubital angiocatheter, followed immediately by a 20-mL continuous saline flush. The multisection image set was acquired every 1-2 sec during the first pass of the contrast agent until 60 time points were obtained.

### Image Processing

Prior to analysis, raw RSI data were corrected for geometric distortions due to susceptibility, gradient nonlinearities, and eddy currents.<sup>13</sup> This was followed by correction of patient motion using in-house software. ADC values were calculated from a tensor fit to the full

dataset (all  $b$ -values and diffusion directions). The RSI model and analysis are detailed in White et al.<sup>11</sup> Briefly, the diffusion signal in each voxel was fit using a linear mixture model of restricted and hindered water compartments with spherical and cylindrical geometries. For this analysis, the resulting spherically-restricted water fraction formed the basis of our RSI maps. To maximize sensitivity and specificity to the spherically-restricted water fraction, a beamforming filter was applied to our RSI maps to reduce residual signal contamination from cylindrically-restricted and hindered water compartments.<sup>11</sup>

DSC perfusion data was post-processed using previously published methods<sup>14</sup> and commercially available software (NordicICE Perfusion Analysis module, NordicNeuroLab, Bergen, Norway), and normalized  $T_1/T_2$  leakage corrected rCBV maps were generated.

RSI maps and rCBV maps were then co-registered in order to assess the rCBV within the regions of restricted diffusion in both the patients with BRIA as well as in the GBM controls.

## ROIs

Volumetric ROIs were drawn manually on the RSI maps to delineate the region of restricted diffusion for both the patient group with BRIA as well as for the control group with treatment-naïve GBM. This was done using the Amira<sup>®</sup> software package (Visage Imaging, Inc.). For each patient, the entire area of restricted diffusion was included, i.e. all voxels which demonstrated high signal intensity on the RSI map were included in the ROI. NAWM ROI's were also drawn within the white matter contralateral to the area of restricted diffusion on the 3D FLAIR sequence. All manual ROIs were drawn by two board-certified neuroradiologists, both with 3 years of experience prior to image analysis.

## Statistical Analysis

Due to the small sample size and non-normal distribution of the data, Mann-Whitney U tests were used to test for group differences in RSI and rCBV between the patients with BRIA and the GBM controls. Wilcoxin rank-sum tests were used to test for differences between areas of restricted diffusion and NAWM within each of the groups.

## Results

RSI values in regions of restricted diffusion were significantly higher than in NAWM both for patients with BRIA [ $z(13) = -2.52$ ,  $p = .012$ ] as well as for patients with tumor [ $z(13) = -2.20 = .028$ ]. Moreover, RSI values were higher in the patients with BRIA than in the patients with tumor [ $U(13) = 8.0$ ,  $p = .039$ ]. Conversely, rCBV values within the regions of restricted diffusion were very low in patients with BRIA--lower than in patients with tumor [ $U(9) = 1$ ,  $p = .019$ ] as well as lower than in NAWM [ $z(9) = -2.2$ ,  $p = .028$ ]. In our patient sample, there was only a trend for rCBV values in patients with tumor to be higher than rCBV in NAWM [ $z(9) = -1.46$ ,  $p = .068$ ].

Figure 2 demonstrates these results with a graphical representation of the individual RSI and rCBV values for patients with BRIA, patients with tumor, as well as for the NAWM. Figure 3 also illustrates these results with a direct comparison of two patients with GBM--one

treated with chemoradiation and bevacizumab and the other without any treatment prior to the acquisition of these images. The degree and homogeneity of restricted diffusion is greater in the patient treated with bevacizumab than in the pre-treatment GBM control. Furthermore, the rCBV maps demonstrate that the rCBV in the region of restricted diffusion is remarkably low in the patient treated with bevacizumab—not only lower than rCBV in the GBM control but also lower than in the contralateral NAWM.

Neuropathologic data from subsequent autopsy was available for 2 of the 8 patients (25%) with BRIA, both of which showed similar results. Sections taken from the areas corresponding to the diffusion restriction, as highlighted in Figure 4, revealed areas of eosinophilic coagulative necrosis, hyalinized blood vessels, reactive astrocytosis/gliosis, and scattered atypical gemistocytes. Due to the presence of the scattered atypical gemistocytes, Ki-67 immunostains were performed and found to be entirely negative (Figure 3D), confirming that there was no evidence of proliferating, recurrent tumor.

## Discussion

Previous studies have described the development of a unique type of necrosis, characterized by marked and persistent restricted diffusion, in a subset of patients with malignant glioma treated with bevacizumab<sup>5-7</sup>. This phenomenon has complicated diagnostic and treatment-related decisions in these patients, since recurrent tumor is also associated with restricted diffusion<sup>8,9</sup>. Furthermore, recent studies have highlighted the role of bevacizumab in the treatment of radiation necrosis both following standard radiation therapy for malignant glioma as well as following stereotactic radiosurgery for brain metastases<sup>15,16</sup>. Although these findings appear to be contradictory, they highlight the fact that the necrosis associated with BRIA is different than that associated with radiation therapy alone.

Prior reports have relied on standard DWI/ADC to determine the nature of these areas of restricted diffusion<sup>5-7</sup>. In the present study, we describe this same phenomenon using a recently developed, advanced diffusion-weighted technique called RSI. RSI has shown greater sensitivity to restricted diffusion compared to standard DWI/ADC because it utilizes multiple *b*-values and diffusion times to separate out the spherically restricted water compartment from the hindered water compartment.<sup>10</sup> Using both RSI and rCBV, we demonstrate that patients with BRIA show higher signal on RSI coupled with lower rCBV relative to patients with pathology-confirmed GBM. However, whereas RSI values were on average one and a half times greater in patients with BRIA relative to patients with tumor, rCBV values in these patients were nearly five times lower than in patients with tumor and were even lower than those seen in NAWM. These results suggest that while RSI is very useful in detecting pathology and differentiating abnormal tissue from NAWM, its ability to discriminate BRIA from tumor is less than DSC perfusion as the rCBV values demonstrate a much larger magnitude of difference when comparing these entities. On the other hand, in our patient sample, rCBV values in tumor were not significantly higher than those in NAWM indicating that the ability of rCBV to detect the presence of pathology is less than RSI. These conclusions underscore the complementary nature of these two imaging modalities, with RSI clearly demonstrating the restricted diffusion associated with these pathologies and rCBV better at distinguishing the type of pathology (i.e., tumor vs. BRIA).

The perfusion characteristics of BRIA are not unexpected with the low rCBV values reflecting the anti-VEGF properties of bevacizumab. However, the diffusion characteristics of BRIA are less well understood since DWI/ADC has previously been validated as a biomarker for human glioma cellularity<sup>17</sup>. However, in the case of BRIA neither DWI/ADC nor RSI are reflecting tumor cellularity. This raises the question of why this particular type of necrosis demonstrates such marked restricted diffusion which persists over time, especially since it is well established that typical radiation necrosis actually facilitates diffusion due to liquefaction within the area of necrosis.<sup>18</sup> We propose that due to the anti-VEGF properties of bevacizumab which not only reduces the number of vessels within the tumor bed but also leads to fibrosis and hyalinization of the remaining vessels, macrophages that would normally remove the cells that have undergone necrosis due to radiation can no longer access the area of radiation necrosis. As a result, so-called “ghost cells” remain in the irradiated tumor bed<sup>19</sup>—cells which are characterized by relatively intact plasma membranes filled with cytoplasm but devoid of nuclei or organelles. These cells will restrict diffusion due to their intact plasma membranes and the intrinsically high T2 of their cytoplasm, and this restriction will persist as macrophages cannot access the area to remove them. Further investigation with animal models is underway in our laboratory in order to test this theory.

In addition to demonstrating BRIA in patients with high-grade glioma, as has been done in prior studies<sup>5-7</sup>, the current study also demonstrates this phenomenon in patients with brain metastases treated with bevacizumab. This highlights the essential contribution of radiation therapy to the development of BRIA since patients with both high-grade glioma and brain metastases undergo radiation therapy, whereas the chemotherapeutic regimen of these two patient groups varies greatly.

Neuropathologic data in our study is very similar to the prior studies with a recurring theme of coagulative necrosis and fibrotic, hyalinized blood vessels. We also found scattered areas of gliosis with many reactive gemistocytes. Some gemistocytes, particularly those around blood vessels, had an atypical appearance. However, we utilized Ki-67 immunostains in both of the cases for which histology was available. This allowed us to verify that none of the scattered atypical cells were proliferating tumor cells, but rather likely represented reactive cells.

Limitations of our study include the small sample size, lack of perfusion data for a subset of the patients and controls, and histologic validation for only 25% of our patient group. Furthermore, the neuropathologic data for the 2 patients with BRIA came from subsequent autopsy, resulting in inherent pre-selection bias. However, follow-up MRI's were available for all of the patients with BRIA and demonstrated that the restricted diffusion persisted on average 8 months and up to 16 months in duration, further corroborating the assumption that these lesions were related to bevacizumab therapy rather than recurrent tumor.

In conclusion, we show that by combining the ability of RSI to detect pathology and differentiate it from NAWM and the ability of DSC perfusion to clearly distinguish the high rCBV of tumor from the remarkably low rCBV of BRIA, we can increase our diagnostic certainty in discriminating areas of bevacizumab-related necrosis from recurrent tumor.



## Acknowledgments

NIH grants R01NS065838 (C.R.M.), RC2 DA29475 (A.M.D.) and EB00790-06 (A.M.D.) and 3P30CA023100-25S8 (S.K.), CAPES for PhD student scholarship (D.B.A.F)

## References

1. Friedman HS, Prados MD, Wen PY, et al. Bevacizumab alone and in combination with irinotecan in recurrent glioblastoma. *J Clin Oncol.* 2009; 27:4733–40. [PubMed: 19720927]
2. Soffietti R, Trevisan E, Ruda R. Targeted therapy in brain metastasis. *Curr Opin Oncol.* 2012; 24:679–86. [PubMed: 22820413]
3. Schettino C, Bareschino MA, Rossi A, et al. Targeting angiogenesis for treatment of NSCLC brain metastases. *Curr Cancer Drug Targets.* 2012; 12:289–99. [PubMed: 22229249]
4. Hygino da Cruz LC Jr, Rodriguez I, Domingues RC, et al. Pseudoprogression and pseudoresponse: imaging challenges in the assessment of posttreatment glioma. *AJNR Am J Neuroradiol.* 2011; 32:1978–85. [PubMed: 21393407]
5. Jeyaretna DS, Curry WT Jr, Batchelor TT, et al. Exacerbation of cerebral radiation necrosis by bevacizumab. *J Clin Oncol.* 2011; 29:e159–62. [PubMed: 21149667]
6. Mong S, Ellingson BM, Nghiemphu PL, et al. Persistent diffusion-restricted lesions in bevacizumab-treated malignant gliomas are associated with improved survival compared with matched controls. *AJNR Am J Neuroradiol.* 2012; 33:1763–70. [PubMed: 22538078]
7. Rieger J, Bahr O, Muller K, et al. Bevacizumab-induced diffusion-restricted lesions in malignant glioma patients. *J Neurooncol.* 2010; 99:49–56. [PubMed: 20035366]
8. Kono K, Inoue Y, Nakayama K, et al. The role of diffusion-weighted imaging in patients with brain tumors. *AJNR Am J Neuroradiol.* 2001; 22:1081–8. [PubMed: 11415902]
9. Sugahara T, Korogi Y, Kochi M, et al. Usefulness of diffusion-weighted MRI with echo-planar technique in the evaluation of cellularity in gliomas. *J Magn Reson Imaging.* 1999; 9:53–60. [PubMed: 10030650]
10. White NS, Leergaard TB, D'Arceuil H, et al. Probing tissue microstructure with restriction spectrum imaging: histological and theoretical validation. *Hum Brain Mapp.* 2013; 34:327–46. [PubMed: 23169482]
11. White NS, McDonald CR, Farid N, et al. Improved conspicuity and delineation of primary and metastatic brain tumors using “restriction spectrum imaging”: quantitative comparison with high b-value DWI and ADC. *AJNR Am J Neuroradiol.* 2013; 34:958–64. [PubMed: 23139079]
12. Kothari PD, White NS, Farid N, et al. Longitudinal restriction spectrum imaging is resistant to pseudoresponse in patients with high-grade gliomas treated with bevacizumab. *AJNR Am J Neuroradiol.* 2013; 34:1752–7. [PubMed: 23578667]
13. Holland D, Kuperman JM, Dale AM. Efficient correction of inhomogeneous static magnetic field-induced distortion in Echo Planar Imaging. *Neuroimage.* 2010; 50:175–83. [PubMed: 19944768]
14. Emblem KE, Bjornerud A. An automatic procedure for normalization of cerebral blood volume maps in dynamic susceptibility contrast-based glioma imaging. *AJNR Am J Neuroradiol.* 2009; 30:1929–32. [PubMed: 19628627]
15. Boothe D, Young R, Yamada Y, et al. Bevacizumab as a treatment for radiation necrosis of brain metastases post stereotactic radiosurgery. *Neuro Oncol.* 2013; 15:1257–63. [PubMed: 23814264]
16. Sadraei NH, Dahiya S, Chao ST, et al. Treatment of cerebral radiation necrosis with bevacizumab: the Cleveland Clinic experience. *Am J Clin Oncol.* 2013 [Epub ahead of print].
17. Ellingson BM, Malkin MG, Rand SD, et al. Validation of functional diffusion maps (fDMs) as a biomarker for human glioma cellularity. *J Magn Reson Imaging.* 2010; 31:538–48. [PubMed: 20187195]
18. Shah R, Vattoth S, Jacob R, et al. Radiation necrosis in the brain: imaging features and differentiation from tumor recurrence. *Radiographics.* 2012; 32:1343–59. [PubMed: 22977022]
19. Yoshii Y. Pathological review of late cerebral radionecrosis. *Brain Tumor Pathol.* 2008; 25:51–8. [PubMed: 18987829]

## Abbreviation Key

<b>BRIA</b>	bevacizumab-related imaging abnormality
<b>GBM</b>	glioblastoma multiforme
<b>NAWM</b>	normal-appearing white matter
<b>NSCLC</b>	non-small cell lung cancer
<b>rCBV</b>	relative cerebral blood volume
<b>RSI</b>	restriction spectrum imaging
<b>VEGF</b>	vascular endothelial growth factor



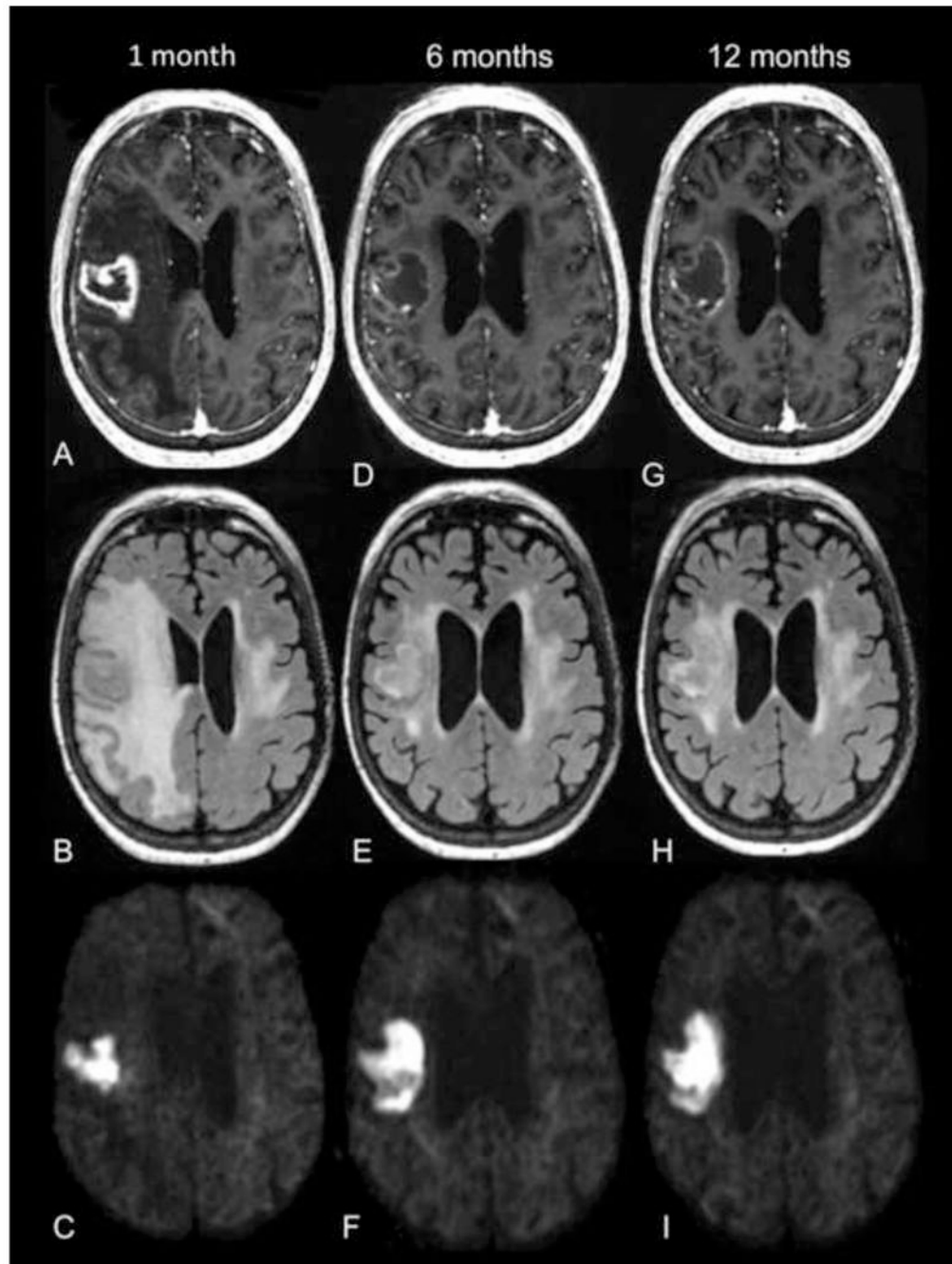


**Figure 1.**

72 year old female with brain metastasis from NSCLC. T1 post-contrast (first row), FLAIR (second row), and RSI (third row) images are shown from 1 month (A-C), 6 months (D-F), and 12 months (G-I) after initiation of bevacizumab therapy. Contrast enhancement and surrounding FLAIR hyperintensity significantly decrease on the 6 and 12 month follow-up scans. However, the region of marked restricted diffusion on the RSI map increases in size on the 6 month follow-up scan and persists at 12 months.

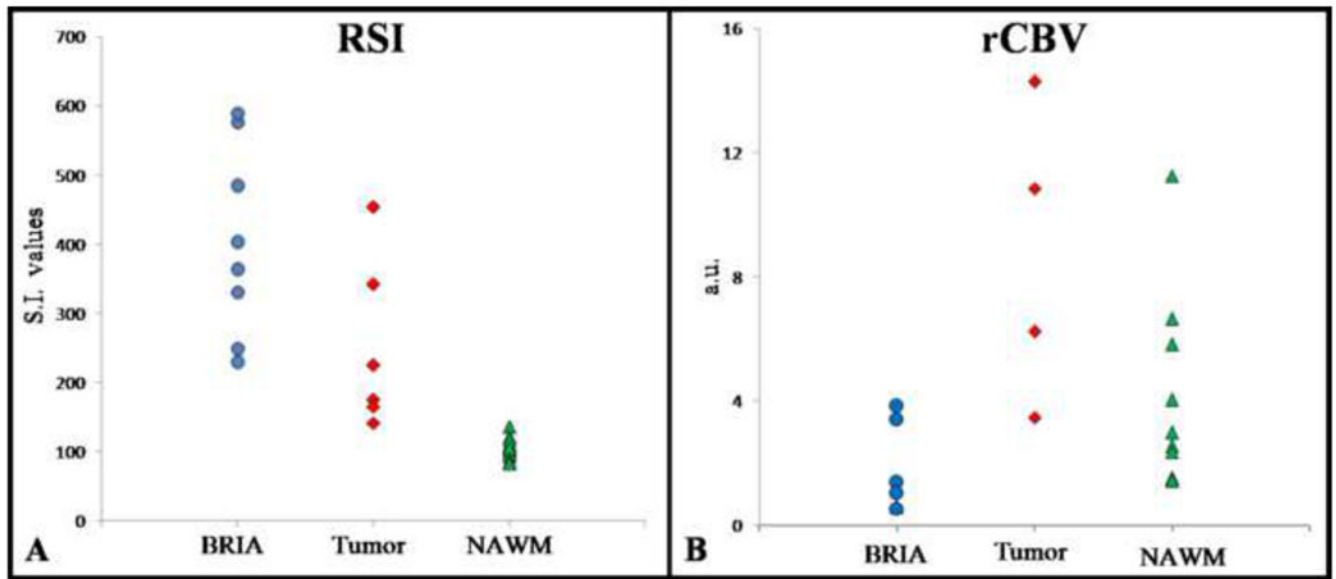


**Figure 2.**

Plot of individual RSI (A) and normalized rCBV (B) values for each of the patients with BRIA and tumor, as well as for NAWM. RSI values are displayed as signal intensity (S.I.) values, and rCBV values are displayed as arbitrary units (a.u.). RSI data is available for all patients with BRIA and all GBM controls (8 and 6, respectively), whereas rCBV data is available for 6 of the patients with BRIA and 4 of the GBM controls. While the RSI values for patients with BRIA are higher than for those with tumor, rCBV values demonstrate a much larger magnitude of difference between these entities.

\* Please note, two of the data points for the patients with BRIA on the rCBV graph are overlapping due to very similar numerical values (0.55 and 0.59 a.u.).

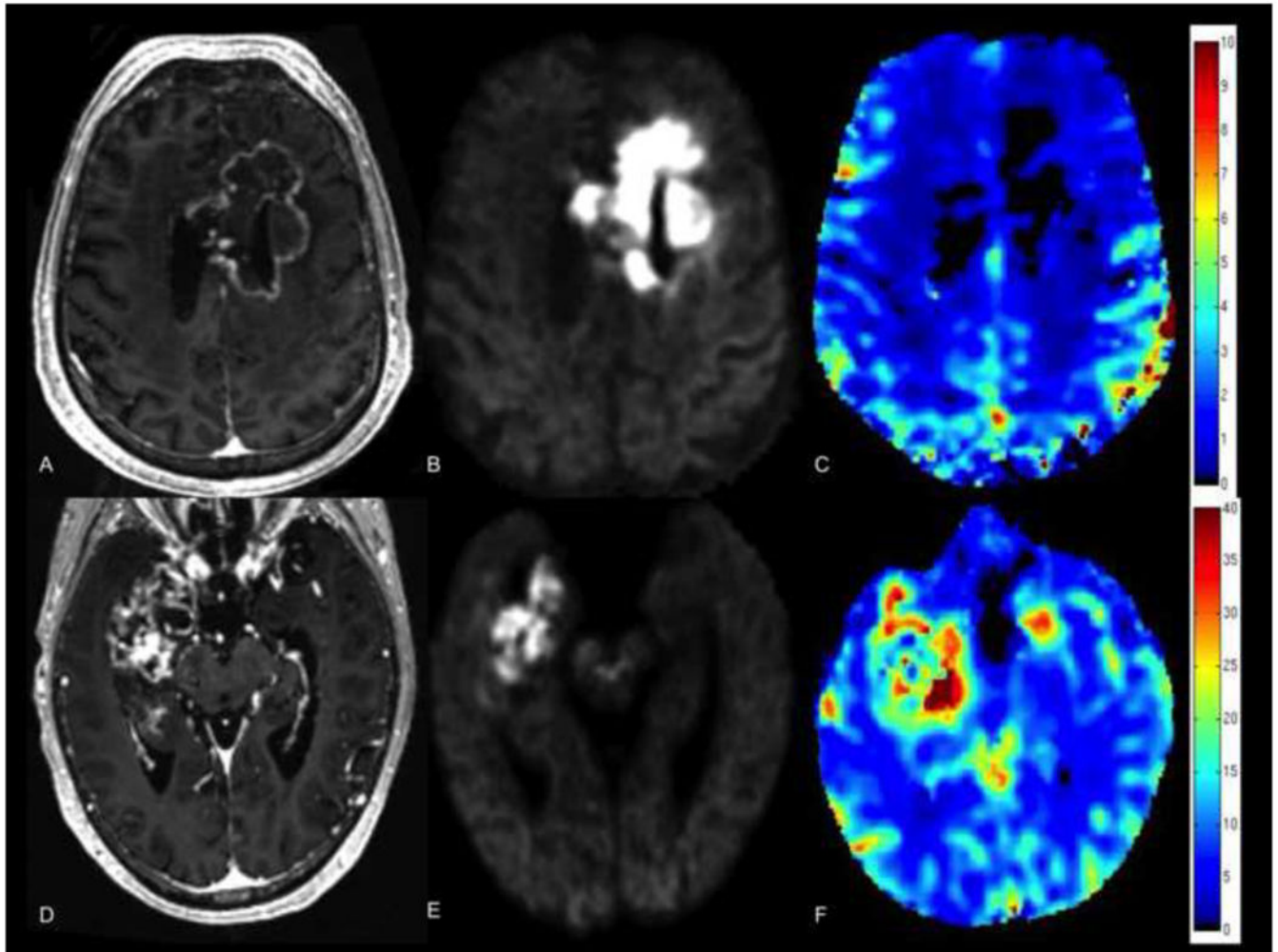


**Figure 3.** Comparison of 55 year old male with GBM treated with chemoradiation and bevacizumab (top row) and 66 year old male with GBM prior to any treatment (bottom row). T1 post-contrast images (A, D), RSI maps (B, E), and rCBV maps (C, F) are shown. Degree and homogeneity of restricted diffusion is greater in the patient treated with bevacizumab than in the pre-treatment GBM control (images scaled identically with same window and level), whereas rCBV in the region of restricted diffusion is remarkably low in the patient treated with bevacizumab—lower than in the GBM control and lower than in the NAWM.

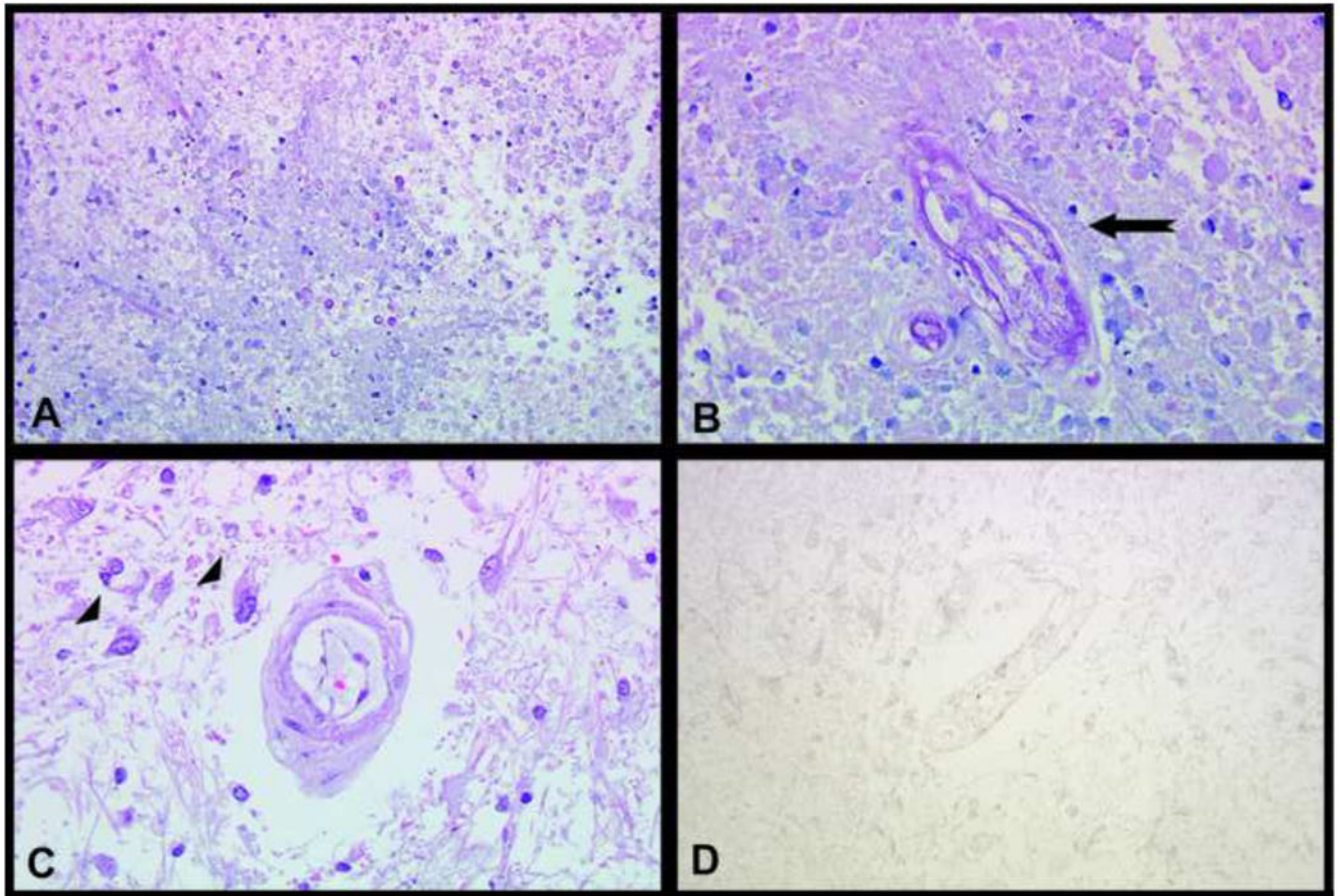


**Figure 4.** Micrographs of brain autopsy tissue from two patients with bevacizumab-treated GBM. Hematoxylin and eosin (H&E) stained sections (A-B) from an area of restricted diffusion demonstrate eosinophilic coagulative necrosis, necrotic/hyalinized blood vessels (arrow in B), and a few dystrophic calcifications. An H&E stained section (C) from another area of restricted diffusion shows scattered atypical gemistocytes adjacent to a hyalinized vessel (arrowheads in C) on a background of gliotic white matter. Ki-67 immunostain (D) corresponding to the H&E stain from part C is entirely negative. (A: 200×, B,C,D: 400× magnifications)



Table 1

## Patients Characteristics

Patient	Age/Gender <sup>a</sup>	Pathology <sup>b</sup>	Radiation therapy <sup>c</sup>	Chemotherapy <sup>d</sup>	Length of time with BRIA <sup>e</sup>
1	44/F	GBM	Hypofractionated XRT; subsequent SRS	TMZ, Sirolimus, Erlotinib	11 mo
2	55/M	GBM	Standard fractionated XRT	TMZ, Nilotinib	16 mo
3	58/M	GBM	Standard fractionated XRT	TMZ, Irinotecan, Carboplatin	5 mo
4	62/M	GBM	Standard fractionated XRT	TMZ	10 mo
5	45/M	AA	Standard fractionated XRT	TMZ, Lomustine	9 mo
6	29/F	AA	Standard fractionated XRT	TMZ, Carboplatin	2 mo
7	72/F	Met (NSCLC)	SRS	Systemic	12 mo
8	79/M	Met (Melanoma)	SRS	Systemic	2 mo

<sup>a</sup>F = female, M = male

<sup>b</sup>GBM = glioblastoma, AA = anaplastic astrocytoma, Met = Metastasis

<sup>c</sup>XRT = radiation therapy, SRS = stereotactic radiosurgery

<sup>d</sup>TMZ = temozolomide

<sup>e</sup>BRIA = bevacizumab-related imaging abnormality